ELSEVIER

Polymer 40 (1999) 1241–1250

polymer

Hard-sphere-chain equations of state for lyotropic polymer liquid crystals

Toshiaki Hino[a,b], John M. Prausnitz[a,b,*]

[a]Department of Chemical Engineering, University of California, Berkeley, CA 94720, USA
[b]Chemical Sciences Division, Lawrence Berkeley National Laboratory, University of California, Berkeley, CA 94720, USA

Received 16 December 1997; accepted 25 March 1998

Abstract

Using Parsons-type scaling, the Onsager theory for the isotropic–nematic (I–N) transition of rigid-rod lyotropic polymer liquid crystals is combined with the equation of state for hard-sphere-chain fluids of Chapman et al. and that of Hu et al. The equation of Hu et al. gives the I–N transition pressure and density in good agreement with computer simulation by Wilson and Allen for a semi-flexible hard-sphere chain consisting of seven segments. For real semi-flexible polymers, we follow the Khokhlov–Semenov theory of persistent chains that introduces chain flexibility into the Onsager theory. Using a consistent procedure to regress the equation-of-state parameters, the equations of Chapman et al. and Hu et al. are also compared with the theory of DuPré and Yang that uses the equation of Lee for hard spherocylinders. These models are compared with experiment for two binary polymer solutions containing poly(hexyl isocyanate) and another solution containing polysaccharide schizophyllan. The concentration of polymer at the I–N transition is predicted as a function of the molecular weight of polymer. All models perform similarly and show semi-quantitative agreement with experiment.

Keywords: Equation of state; Lyotropic polymer liquid crystals; Onsager theory

---

1. Introduction

In good solvents, lyotropic polymer liquid crystals exhibit the isotropic–nematic (I–N) transition as the concentration of polymer rises [1]. There has been continuing interest in the theoretical description of the I–N transition of lyotropic polymer liquid crystals [1–3]. For lyotropic polymer liquid crystals, the Flory [1] and Onsager [1–3] theories are widely used to compute the I–N transition of rodlike molecules. In this work, we consider the Onsager theory of lyotropic polymer liquid crystals where the I–N transition results from the competition between the orientational entropy and the entropy associated with the excluded volume that favor, respectively, the disordered isotropic phase and the ordered nematic phase.

Molecular thermodynamic models for lyotropic polymer liquid crystals use the equation-of-state theory for hard particles such as hard spherocylinders. Among them, the particularly simple yet accurate model of Lee [4–6] applies the scaling approach of Parsons [7] to hard spherocylinders. By decoupling translational degrees of freedom from orientational degrees of freedom, the Parsons scaling theory introduces both molecular orientation and molecular shape into the Helmholtz energy for a hard-sphere fluid [7,8]; the Helmholtz energy for hard-spherocylinder fluids is obtained by scaling the Helmholtz energy for hard-sphere fluids [4–6]. For the I–N transition of hard spherocylinders, Parsons' theory shows good agreement with computer simulations [8].

Recently, a group of new equations of state has appeared for hard-sphere-chain fluids [9–15] where a molecule is represented by a chain of tangent hard spheres. Hu et al. [13] compared several equation-of-state theories for hard-sphere chains with computer simulations. To predict the I–N transition of hard-sphere-chain fluids, Vega and Lago [16] and later Williamson [17] used Parsons-type scaling by combining the equation of state for hard-sphere chains by Chapman et al. [10] with the Onsager theory. The equation of Chapman et al. [10] is based on the theory of associating fluids due to Wertheim [9]. The equation of Chapman et al. is most suitable for linear tangent hard-sphere chains (i.e. hard-sphere chains in a linear configuration) [10,12]. The Parsons-type scaling used by Vega et al. introduces the orientational effect into the equation of state for hard-sphere chains through the second virial coefficient [16,17].

Boublík has indicated that, for isotropic fluids, compressibility factors of flexible hard-sphere chains are very close to those of linear tangent hard-sphere chains [12]. Indeed, at

---

[*] Corresponding author.

0032-3861/98/$ - see front matter
PII S0032-3861(98)00265-1

moderate packing fractions, the equation of Chapman et al. and the other equations presented in Refs. [9–15] give similar compressibility factors in good agreement with computer simulations for flexible hard-sphere chains [13].

However, differences among the equations of state for hard-sphere chains become noticeable in the second virial coefficient as the chain length rises [13]. Because the Parsons-type scaling used by Vega et al. [16,17] introduces the orientational effect through the second virial coefficient, we here examine how the choice of the equation of state for hard-sphere chains affects the predicted I–N transition. Among several equations shown in Ref. [13], the equation of Chapman et al. [10] and that of Hu et al. [13] give, respectively, the largest and smallest second virial coefficients for hard-sphere chains. In this work, we combine the equation of state for hard-sphere chains of Chapman et al. [10] and that of Hu et al. [13] with the Onsager theory to compute the I–N transition.

The equation of Hu et al. shows excellent agreement with computer simulations for both second virial coefficients and compressibility factors of flexible hard-sphere chains over a wide range of chain length [13]. To combine the equation of Hu et al. with the Onsager theory, we follow closely the Parsons-type scaling proposed by Vega and Lago [16,17]. We first compare the equation of Hu et al. [13] and that of Chapman et al. [10] with the computer simulation by Wilson and Allen for a fairly rigid semi-flexible hard-sphere chain consisting of seven segments [18].

For real semi-flexible polymers, it is necessary to introduce chain flexibility into the orientational entropy of the Onsager theory [1–3,5,6]. For the orientational entropy of semi-flexible polymers, we use the equation of DuPré and Yang [5] that is based on the theory of Khokhlov and Semenov for persistent chains [19].

We compare theory with experiment for two binary polymer solutions containing poly(hexyl isocyanate) [20,21] and for another solution containing polysaccharide schizophyllan [22,23]. Using a consistent procedure to regress the equation-of-state parameters, the equation of Chapman et al. and that of Hu et al. are also compared with the model of DuPré and Yang [5] that uses the equation of Lee for hard spherocylinders [4–6]. For representing semi-flexible polymers, each model requires two equation-of-state parameters that represent the size of the molecule. These parameters are regressed from osmotic-pressure data for isotropic solutions [20,22]. For the orientational entropy in the nematic phase, theory also requires the persistence length that defines the extent of chain flexibility. For each solvent-polymer pair, we use the reported persistence length that was regressed from intrinsic-viscosity data by the wormlike-chain theory [21,23]. Using three parameters, we then predict the concentration of polymer at the I–N transition as a function of polymer molecular weight.

2. Theoretical framework

2.1. Parsons-type scaling applied to the Onsager theory

For athermal systems where the attractive interaction is negligible, the Onsager theory expresses the residual Helmholtz energy of rigid rod/solvent systems as a sum of the orientational entropy and the orientation-dependent second virial coefficient (i.e. excluded volume) using a single-particle orientational distribution function [1–3]. The I–N transition follows the competition between the orientational entropy and the entropy associated with the excluded volume that favor, respectively, the disordered isotropic phase and the ordered nematic phase. The Onsager theory predicts that the isotropic phase is stable at low rod concentrations. As the rod concentration rises, a biphasic region appears where the isotropic and nematic phases coexist. At higher rod concentrations, the nematic phase becomes the only stable phase.

In the Onsager theory, a binary rigid rod/solvent system is represented by a pseudo one-component system using the equation-of-state theory. In that representation, thermodynamic properties of the mixture are expressed in terms of the packing fraction of rigid rod and the equation of state gives the osmotic pressure of the solution. Various improvements in the Onsager theory have been proposed to extend the theory to higher concentrations where the truncated second-virial-coefficient expansion is not sufficient [1–3].

To extend the Onsager theory to higher concentrations and to other hard particles such as hard-sphere chains, we use Parsons-type scaling as proposed by Vega et al. [16,17]. In the nematic phase, this scaling introduces the effect of molecular orientation into the equation of state for hard particles through the second virial coefficient. In Parsons-type scaling of Vega et al., the equation of state of the anisotropic phase is expressed in terms of that of the isotropic phase; the essential step is the assumption [16,17]

$$\frac{B_i^{\text{aniso}}}{B_i^{\text{iso}}} = \frac{B_2^{\text{aniso}}}{B_2^{\text{iso}}}, \tag{1}$$

where B_i^{iso} and B_i^{aniso} are the ith virial coefficient of the isotropic phase and that of the anisotropic (i.e. nematic) phase, respectively.

Consider a system of volume V containing N molecules of volume v_0. Under the assumption of Eq. (1), the compressibility factor and the Helmholtz energy per molecule of the anisotropic phase are given in terms of the compressibility factor of the isotropic phase [16,17]:

$$Z_{\text{aniso}} = 1 + \left(\frac{B_2^{\text{aniso}}}{B_2^{\text{iso}}}\right)(Z_{\text{iso}} - 1) \tag{2}$$

$$\frac{A_{\text{aniso}}}{kT} = \frac{A_0}{kT} + \ln \eta + \sigma + \left(\frac{B_2^{\text{aniso}}}{B_2^{\text{iso}}}\right) \int_0^{\eta} \frac{Z_{\text{iso}} - 1}{\eta} \mathrm{d}\eta, \tag{3}$$

where k is the Boltzmann constant, T is the absolute temperature, $\eta = N\nu_0/V$ is the packing fraction (i.e. reduced density), Z_{iso} is the compressibility factor of the isotropic phase, A_0 is the Helmholtz energy per molecule in the standard state, and σ is the negative of the orientational entropy per molecule. The standard state is the ideal isotropic solution where $Z_{\mathrm{iso}} = 1$ and $\sigma = 0$ at unit packing fraction.

In Eqs. (2) and (3), σ and B_2^{aniso} depend on the single-particle orientational distribution function. Specifically, B_2^{aniso} is a function of parameter ρ that is proportional to the average of the sine of the angle between two molecular-orientation vectors. Parameters σ and ρ are defined by

$$\sigma(f) = \int f(\Omega)\ln[4\pi f(\Omega)]\mathrm{d}\Omega \tag{4}$$

$$\rho(f) = \frac{4}{\pi}\int \left|\sin\gamma(\Omega,\Omega')\right| f(\Omega)f(\Omega')d\Omega d\Omega', \tag{5}$$

where f is the single-particle orientational distribution function, Ω is the solid angle and γ is the angle between two molecular-orientation vectors.

With $\sigma = 0$ and $B_2^{\mathrm{iso}} = B_2^{\mathrm{aniso}}$, Eqs. (2) and (3) reduce to the compressibility factor and the Helmholtz energy per molecule, respectively, of the isotropic phase. The Helmholtz energy per molecule of the isotropic phase is given by

$$\frac{A_{\mathrm{iso}}}{kT} = \frac{A_0}{kT} + \ln\eta + \int_0^{\eta} \frac{Z_{\mathrm{iso}} - 1}{\eta}\mathrm{d}\eta. \tag{6}$$

2.2. Semi-flexible polymers

For real semi-flexible polymers, it is necessary to introduce the effect of chain flexibility into the Onsager theory. In this work, we follow the method of DuPré and Yang [5] for semi-flexible polymers based on the Khokhlov–Semenov theory of persistent chains [19]. For semi-flexible polymers, we use the single-particle orientational distribution function in the Onsager theory as the orientational distribution function of unit vectors tangent to the contour of a semi-flexible chain. Chain flexibility has a large effect on the predicted polymer concentration at the I–N transition [5,6].

In this work, we use Onsager's trial function for the single-particle orientational distribution function to compute the orientational entropy σ and parameter ρ for B_2^{aniso}. For semi-flexible polymers, these parameters are given by [2,5]

$$\sigma(\alpha; L/P) \approx \ln\alpha - 1 + \pi e^{-\alpha} + \frac{L}{6P}(\alpha - 1) + \frac{5}{12}\ln\left[\cosh\left(\frac{L}{P}\frac{\alpha - 1}{5}\right)\right] \tag{7}$$

$$\rho \approx \frac{4}{\sqrt{\pi\alpha}}\left[1 - \frac{15}{16\alpha} + \frac{105}{512\alpha^2} + \frac{315}{8192\alpha^3}\right], \tag{8}$$

where α is the variational parameter that specifies the sharpness of the distribution in Onsager's trial function, L is the contour length, and P is the persistence length of polymer. Parameter α is determined by minimizing the Helmholtz energy per molecule of the anisotropic phase. For the nematic phase, $\sigma > 0$ and $\rho < 1$.

In Eq. (7), we recover rigid rods in the limit $L/P \to 0$. Without resorting to Onsager's trial function for the single-particle orientational distribution function, Williamson recently presented a Monte-Carlo annealing technique that determines exactly the orientational distribution function by directly minimizing the Helmholtz energy per molecule of the anisotropic phase [17].

In the present theory, the flexibility parameter L/P enters only in the nematic phase. While the Helmholtz energy of the isotropic phase also depends on this parameter, that dependence is very weak and is neglected here.

2.2.1. Model 1. Equation of Chapman et al. for hard-sphere chains

Recently, several equations of state have appeared for hard-sphere chain fluids [9–15]. Williamson [17] combined the equation of Chapman et al. with Eqs. (2) and (3) to predict the I–N transition. The equation of Chapman et al. [10] is most suitable for hard-sphere chains in a linear configuration (i.e. linear tangent hard-sphere chains) [10,12]. In the equation of Chapman et al., Z_{iso} is given by [10,17]

$$Z_{\mathrm{iso}} = 1 + \frac{r\left(4\eta - 2\eta^2\right)}{(1-\eta)^3} - (r-1)\frac{\left(5/2\eta - \eta^2\right)}{(1-\eta)(1-\eta/2)}, \tag{9}$$

where r is the number of segments per molecule. For B_2^{aniso}, Williamson used the exact expression for the orientation-dependent second virial coefficient of a pair of linear tangent hard-sphere chains given by [24]

$$B_2^{\mathrm{aniso}} = \frac{(11r - 3)}{2r} + \frac{(201)^2(3.4721\pi\rho + 0.191)}{8r}. \tag{10}$$

The equation of Chapman et al. gives $B_2^{\mathrm{iso}} = (3r+5)/2$, close to the second virial coefficient of linear tangent hard-sphere chains in the isotropic phase (i.e. Eq. (10) with $\rho = 1$). In this work, the model that uses Eqs. (9) and (10) is Model 1.

2.2.2. Model 2. Equation of Hu et al. for hard-sphere chains

At moderate packing fractions, equations of state for hard-sphere chain fluids in Refs. [9–15] give similar compressibility factors in good agreement with computer simulations [13]. However, the difference among these equations of state becomes noticeable in the second virial coefficient as the chain length rises [13]. Because Parsons-type scaling as used in this work introduces the effect of molecular orientation through the second virial coefficient, we examine how the choice of equation of state for hard-sphere chains affects the model's predictions of the I–N transition. We propose a semi-empirical procedure to combine any equation of state for hard-sphere chains with Parsons-type scaling as given by Eqs. (2) and (3). To combine the equation-of-state theory with Eqs. (2) and (3), we need the expression for B_2^{aniso} as a function of ρ.

For a pair of linear tangent hard-sphere chains, Eq. (10) shows that B_2^{aniso} consists of the second virial coefficient for a parallel configuration $(11r - 3)/2r$ and a function that is linear in ρ having a small intercept at $\rho = 0$. Therefore, we propose to combine Eqs. (2) and (3) with any equation of state for hard-sphere chains by assuming that B_2^{aniso} is given by

$$B_2^{\text{aniso}} = \frac{(11r-3)}{2r} + \left[B_2^{\text{iso}} - \frac{(11r-3)}{2r}\right]\rho. \tag{11}$$

As an example, we use the equation of state of Hu et al. that gives second virial coefficients and compressibility factors in excellent agreement with computer simulations for flexible hard-sphere chains over a wide rage of chain length [13]. The equation of Chapman et al. gives a second virial coefficient that is consistently larger than that from the equation of Hu et al. for $r > 1$ where r is the number of segments per chain [13]. In the equation of Hu et al., Z_{iso} and B_2^{iso} are given by [13]

$$Z_{\text{iso}} = \frac{1 + a\eta + b\eta^2 - c\eta^3}{(1-\eta)^3} \tag{12}$$

$$B_2^{\text{iso}} = 3 + a, \tag{13}$$

where a, b and c are given by

$$a = r\left(1 + \frac{r-1}{r}a_2 + \frac{r-1}{r}\frac{r-2}{r}a_3\right) \tag{14}$$

$$b = r\left(1 + \frac{r-1}{r}b_2 + \frac{r-1}{r}\frac{r-2}{r}b_3\right) \tag{15}$$

$$c = r\left(1 + \frac{r-1}{r}c_2 + \frac{r-1}{r}\frac{r-2}{r}c_3\right), \tag{16}$$

where

$$a_2 = 0.45696,\ b_2 = 2.10386,\ c_2 = 1.75503,$$

$$a_3 = -0.74745,\ b_3 = 3.49695,\ c_3 = 4.83207. \tag{17}$$

The model that uses Eqs. (11)–(13) is Model 2.

2.2.3. Model 3. Equation of Lee for hard spherocylinders

For the I–N transition of lyotropic polymer liquid crystals, most theories are based on the equation-of-state theory for hard spherocylinders such as the scaled-particle theory [17,25,26]. In this work, we compare Models 1 and 2 for hard-sphere chains with the equation of Lee for hard spherocylinders that is also based on Parsons scaling [4–6].

In the equation of Lee, the effect of molecular shape as well as that of molecular orientation are introduced into the Carnahan–Starling equation of state for hard-sphere fluids. For the anisotropic phase, the compressibility factor and the Helmholtz energy per molecule are given by

$$Z_{\text{aniso}} = 1 + 4\eta\frac{(1-\eta/2)}{(1-\eta)^3}\left[1 + \frac{\rho}{4}g(x)\right] \tag{18}$$

$$\frac{A_{\text{aniso}}}{kT} = \frac{A_0}{kT} + \ln\eta + \sigma + 4\eta\frac{(1-3\eta/4)}{(1-\eta)^2}\left[1 + \frac{\rho}{4}g(x)\right], \tag{19}$$

where x is the aspect ratio of spherocylinder and

$$g(x) = \frac{3x^2/2}{1 + 3x/2}. \tag{20}$$

In Eq. (19), the terms in the square bracket are proportional to the excluded volume of a pair of spherocylinders having angle γ between two molecular-orientation vectors. Hard-sphere fluids are recovered in the limit $x \rightarrow 0$.

In this work, the equation of Lee is Model 3. With $\rho = 1$ and $\sigma = 0$ in Eqs. (18) and (19), we recover the compressibility factor and the Helmholtz energy per molecule of isotropic hard-spherocylinder fluids. Combined with Eqs. (7) and (8), the equation of Lee was also extended to semi-flexible polymers by DuPré and Yang [5].

2.3. Phase equilibrium calculations

Our main interest is to compute the concentration of polymer at the I–N transition. That concentration is obtained from the phase equilibrium conditions for the coexisting isotropic and anisotropic (i.e. nematic) phases at the same temperature:

$$\frac{\mu_{\text{iso}}}{kT} = \frac{\mu_{\text{aniso}}}{kT} \tag{21}$$

$$\frac{\Pi_{\text{iso}}\nu_0}{kT} = \frac{\Pi_{\text{aniso}}\nu_0}{kT} \tag{22}$$

where μ is the chemical potential of polymer, ν_0 is the volume of polymer per molecule and Π is the osmotic pressure. The osmotic pressure represents the chemical potential of solvent. In Eqs. (21) and (22), subscripts iso and aniso denote the isotropic and anisotropic phases, respectively, at the I–N transition.

The chemical potential of polymer and the osmotic pressure depend on parameters σ and ρ defined by Eqs. (7) and (8), respectively. These parameters are functions of the variational parameter α that is determined by the minimization condition

$$\frac{\partial\left(\dfrac{A_{\text{aniso}}}{kT}\right)}{\partial\alpha} = 0. \tag{23}$$

In terms of the compressibility factor and the Helmholtz energy per molecule, the chemical potential of polymer

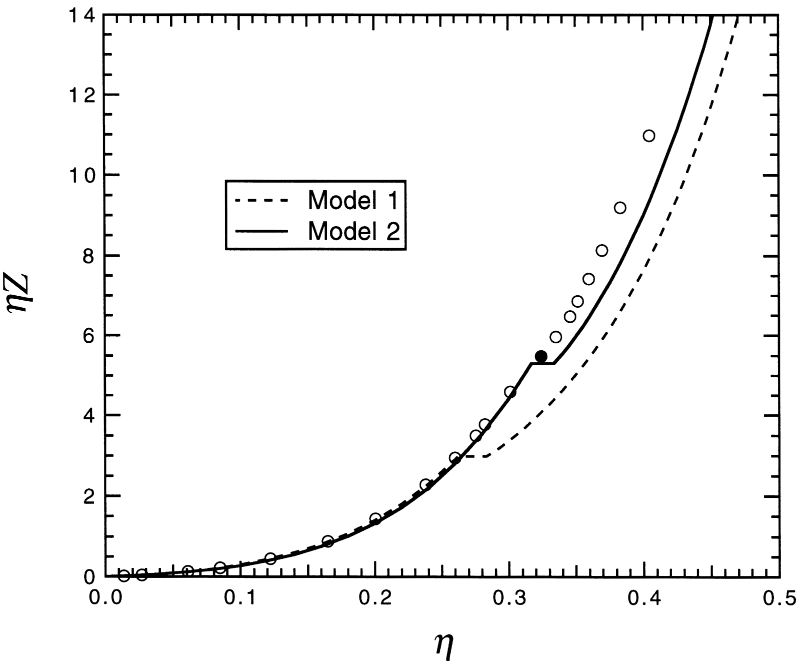

Fig. 1. Reduced pressure ηZ for a hard-sphere chain consisting of seven segments. Open circles represent computer simulation by Wilson and Allen for a nearly rigid semi-flexible hard-sphere chain [18]. The solid circle is the reduced pressure where computer simulation showed the I–N transition. Theoretical curves are for Models 1 and 2 with the orientational entropy for the rigid rod [i.e. $L/P = 0$ in Eq. (7)]. Models 1 and 2 predict the I–N transitions at the pressures where the theoretical curves are displaced toward higher packing fractions.

and the osmotic pressure are given by

$$\frac{\mu}{kT} = \frac{A}{kT} + Z - 1 \tag{24}$$

$$\frac{\Pi v_0}{kT} = \eta Z, \tag{25}$$

where the product of η and Z in Eq. (25) gives a reduced pressure.

3. Comparison with computer simulations

We first compare Models 1 and 2 with computer simulation by Wilson and Allen [18] for a semi-flexible hard-sphere chain consisting of seven segments. For $r = 7$, Models 1 and 2 give $B_2^{\mathrm{iso}} = 13$ and 9.5, respectively. In the simulation by Wilson and Allen, adjacent segments were constrained in narrow potential wells with infinitely steep walls having well width ± 0.05 d where d is the equilibrium bond length. Additional constrains were also applied to prevent non-adjacent spheres from overlapping and to control chain flexibility. For a pair of non-adjacent ith and jth segments, the minimum bond length was set to $|i - j|d$. Therefore, the hard-sphere chains simulated in Ref. [18] are nearly rigid.

Fig. 1 shows the reduced pressure ηZ for a hard-sphere chain consisting of seven segments [18]. Open circles show the computer simulation by Wilson and Allen for a fairly rigid hard-sphere chain [18]. The broken and solid curves are for Models 1 and 2, respectively. Because the hard-sphere chains simulated in Ref. [18] are nearly rigid, theoretical curves were computed using the orientational entropy for the rigid rod [i.e. $L/P = 0$ in Eq. (7)]. The solid circle is the reduced pressure where computer simulation showed the I–N transition. Models 1 and 2 predict the I–N transitions at the pressures where the theoretical curves are displaced toward higher packing fractions.

In the isotropic phase, both Models 1 and 2 show good agreement with computer simulation; there is little difference between Models 1 and 2. The results show that chain flexibility has a very small effect on the reduced pressure of isotropic fluids. Model 2 predicts the I–N transition concentration and pressure in agreement with computer simulation. However, both models overestimate the increase in concentration when the system undergoes the I–N transition.

It is fortuitous that Model 2 predicts the I–N transition concentration and pressure in better agreement with the computer simulation in Ref. [18] than Model 1. The I–N transition concentration is sensitive to the flexibility of hard-sphere chains. As Wilson showed by another set of computer simulations in Ref. [27], the I–N transition concentration rises as chain flexibility increases. Because the primary difference between Models 1 and 2 lies in the second virial coefficient, the curves shown in Fig. 1 only indicate that for Parsons-type scaling, the expression for the second virial coefficient has a large effect on the predicted I–N transition concentration.

In Fig. 1, the disagreement between Model 1 and computer simulations is not due to the use of Onsager's trial function for the orientational distribution function.

Table 1
Equation-of-state parameters for PHIC in DCM at 20°C

	Model 1	Model 2	Model 3
d (Å)	15.0	8.93	12.5
r/M (mol/g)	0.000644	0.00190	0.000903[b]
%rms[a]	2.2	4.1	4.0

[a] Percent root-mean-square relative deviations.
[b] x/M (mol/g).

Table 2
Equation-of-state parameters for PHIC in toluene at 25°C

	Model 1	Model 2	Model 3
d (Å)	9.70	4.23	9.91
r/M (mol/g)	0.00162	0.00818	0.00157[b]
%rms[a]	4.0	3.9	4.4

[a] Percent root-mean-square relative deviations.
[b] x/M (mol/g).

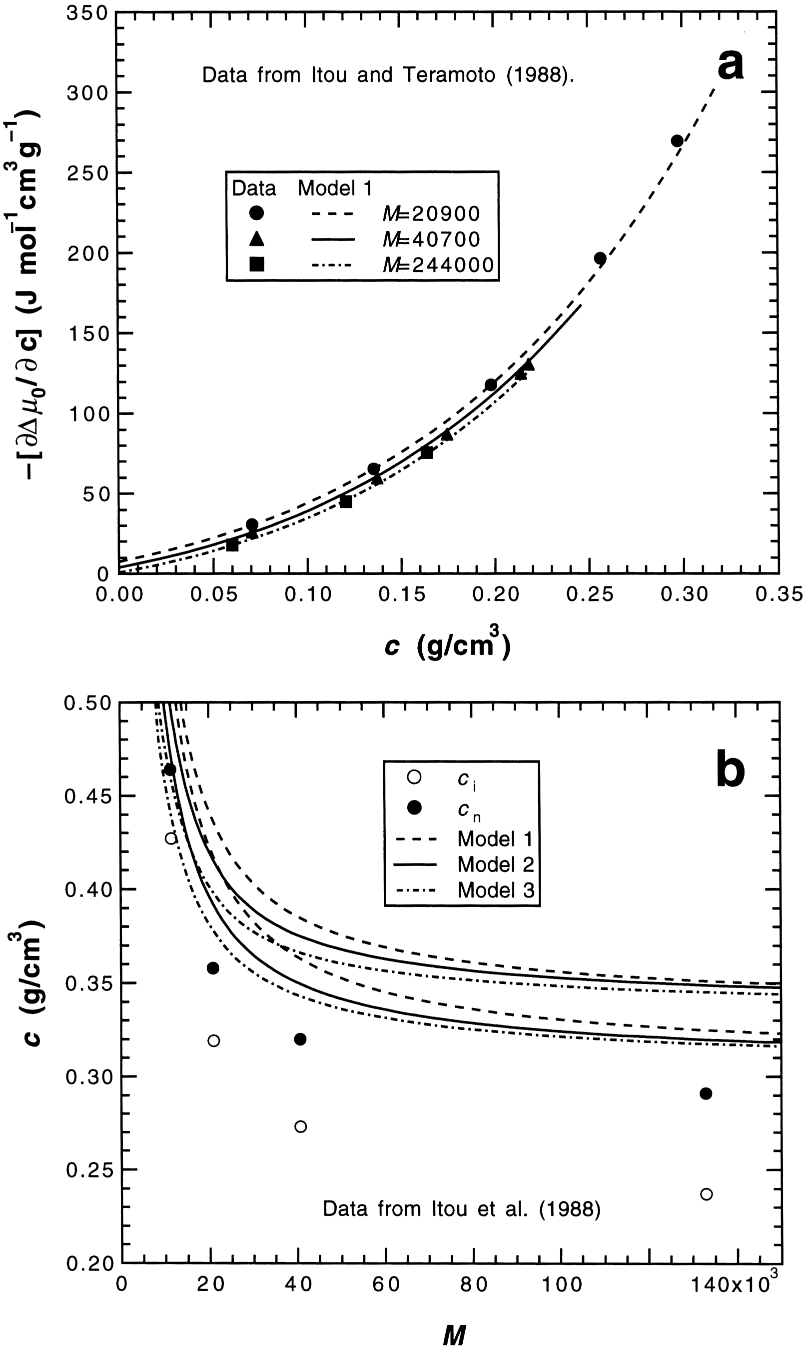

Fig. 2. (a) Derivative of osmotic pressure of isotropic poly(hexyl isocyanate) (PHIC) solutions in dichloromethane (DCM) at 20°C ($\Delta\mu_0 \equiv -\Pi\nu_s$ where ν_s is the volume of solvent per molecule) [20]. Curves are the fit by Model 1 using equation-of-state parameters in Table 1. (b) Polymer concentration at the I-N transition for PHIC in DCM at 20°C [21]. Curves are predictions with $M_L = 740$ g/mol nm and $P = 21$ nm [21] using equation-of-state parameters in Table 1.

There is only a small difference between Model 1 that uses the Onsager's trial function and Model 1 that determines the orientational distribution function exactly by Monte Carlo simulations presented by Williamson [17].

4. Comparison with experiment

We next compare Models 1–3 with experiment for binary polymer solutions that exhibit the I–N transition. Using parameters regressed from experimental properties of isotropic solutions, our objective is to predict the polymer concentration at the I–N transition as a function of polymer molecular weight.

For a given molecular weight of polymer M, Models 1 and 2 use the hard-sphere diameter d and the number of segments per molecule r to specify the size of molecule. Similarly, Model 3 uses hard-spherocylinder diameter d and aspect ratio x. We assume that the equation-of-state parameters d, r/M (for hard-sphere chains), and x/M (for hard spherocylinders) are independent of M. We use the weight-average molecular weight of polymer for M. Polymers studied in this work are monodisperse. For lyotropic polymer liquid crystals, polydispersity has a large effect on the I–N transition [23].

To provide a fair comparison of different models, we regress the equation of state parameters from the same set of experimental data. For each system, these parameters are regressed from the experimental osmotic pressure or from the first derivative of osmotic pressure with respect to polymer concentration in the isotropic phase. The latter thermodynamic property is determined from sedimentation equilibrium measurements. Although both Models 1 and 2 are for hard-sphere chain fluids, the equation-of-state parameters for Model 1 are not necessarily equal to those for Model 2 when these parameters are regressed from experimental data.

To apply Models 1–3 to real systems, it is first necessary to express the packing fraction as a function of the weight fraction of polymer using the measured density of solution. The packing fraction is given by

$$\eta = \left(\frac{w}{\tilde{v}}\right)\left(\frac{\mathrm{N}_{\mathrm{AV}}\nu_0}{M}\right), \tag{26}$$

where w is the weight fraction of polymer, $\tilde{v}$ is the specific volume of solution, N_{AV} is the Avogadro number, ν_0 is the volume of polymer per molecule, and M is the molecular weight of polymer in mass per mole.

For a hard-sphere chain of d and r, ν_0 is given by

$$\nu_0 = \frac{4}{3}\pi\left(\frac{r}{M}\right)\left(\frac{d}{2}\right)^3 M \tag{27}$$

and for a hard spherocylinder of d and x

$$\nu_0 = \pi d^3\left[\frac{1}{4}\left(\frac{x}{M}\right)M + \frac{1}{6}\right]. \tag{28}$$

For semi-flexible polymers, we also need the ratio of contour length L to persistence length P in Eq. (7). Using the contour length per unit mass of polymer M_{L}, L/P is given by

$$L/P = M/(M_{\mathrm{L}}P), \tag{29}$$

where the product of M_{L} and P appears in Eq. (29). For each solvent-polymer pair, we take M_{L} and P from the literature where these parameters are obtained from intrinsic-viscosity data using the wormlike-chain theory [21,23]. Because the persistence length is difficult to determine, the product of M_{L} and P may be used as an adjustable fitting parameter. We use the same persistence length for Models 1–3. In the following, we discuss some systems in the order of decreasing chain flexibility (i.e. in the order of increasing persistence length).

4.1. Poly(hexyl isocyanate) in dichloromethane

We first apply Models 1–3 to poly(hexyl isocyanate) (PHIC) in dichloromethane (DCM) at 20°C [20,21]. For PHIC in DCM at 20°C, Table 1 gives the equation-of-state parameters regressed from sedimentation equilibrium data for isotropic solutions measured by Itou et al. [20]. Percent root-mean-square (%rms) relative deviations between measured and calculated values are also shown in Table 1. Sedimentation equilibrium measurements give the first derivative of osmotic pressure with respect to the concentration of polymer. Based on %rms, Model 1 gives the best fit to the data of Itou et al. [20]. Fig. 2a shows the derivative of osmotic pressure for isotropic PHIC solutions in DCM at 20°C ($\Delta\mu_0 \equiv \Pi\nu_{\mathrm{s}}$ where ν_{s} is the volume of solvent per molecule). Curves are the fit by Model 1.

Fig. 2b shows the polymer concentration at the I–N transition for PHIC in DCM at 20°C. Curves are predictions by Models 1–3 with $M_{\mathrm{L}} = 740$ g/mol nm and $P = 21$ nm [21]. All models predict polymer concentrations at the I–N transition that are higher than experiment, probably because present models overestimate the flexibility effect. Theoretical curves are sensitive to persistence length P. In Fig. 2b, a decrease in P shifts theoretical curves upward. The differences among Models 1–3 are large for polymers with low molecular weights. However, the difference among these models decreases as the polymer molecular weight rises. At the I–N transition, all models underpredict the difference between the concentration of PHIC in the isotropic phase and that in the nematic phase.

4.2. Poly(hexyl isocyanate) in toluene

For PHIC, data are also available for solutions in toluene at 25°C [20,21]. PHIC in toluene is characterized by $M_{\mathrm{L}} = 740$ g/mol nm and $P = 37$ nm [21]. PHIC is stiffer in toluene than in DCM. For PHIC in toluene at 25°C, Table 2 gives the equation-of-state parameters regressed from osmotic-pressure data for isotropic solutions measured by Itou et al. [20]. As reflected in %rms relative deviations,

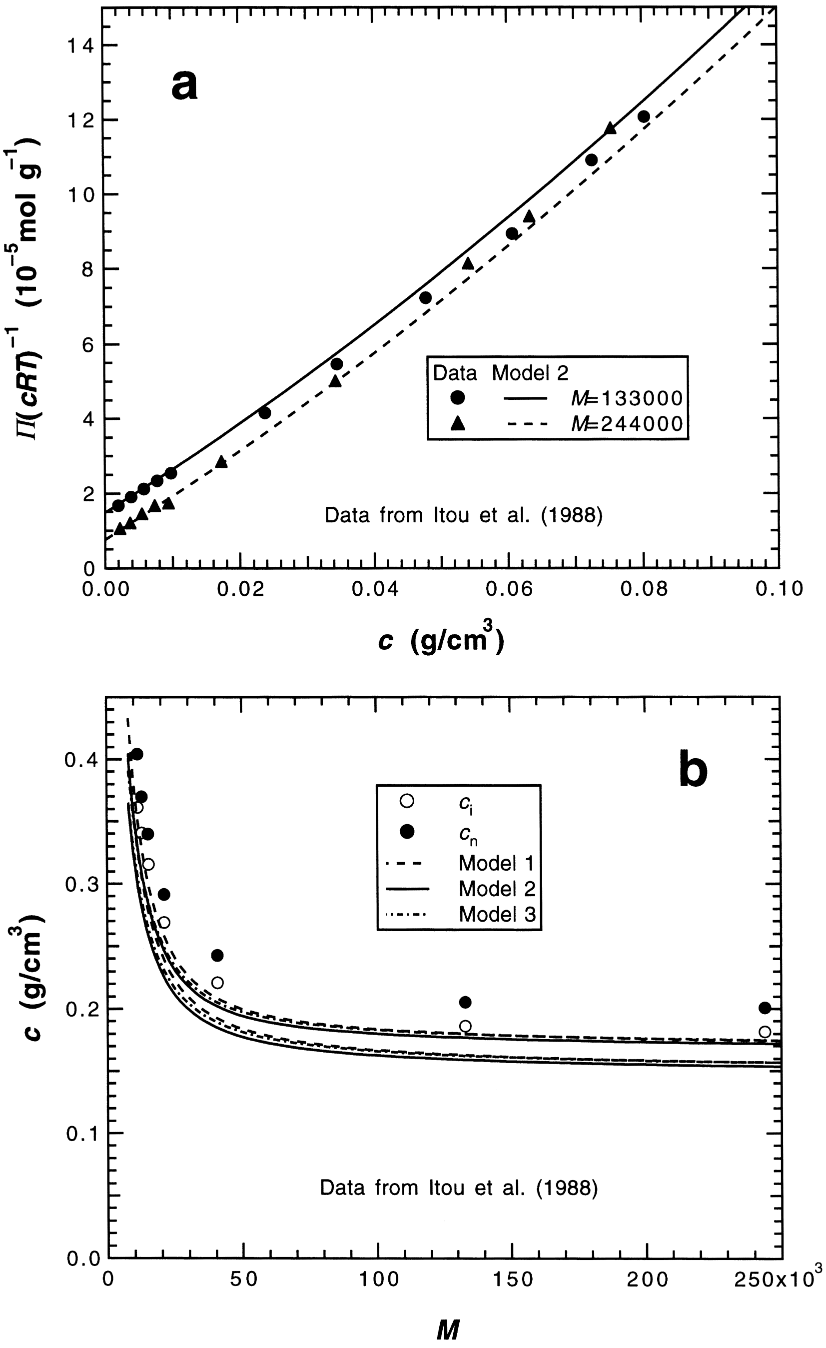

Fig. 3. (a) Osmotic pressure of isotropic poly(hexyl isocyanate) (PHIC) solutions in toluene at 25°C [20]. Curves are the fit by Model 2 with the equation-of-state parameters given in Table 2. (b) Polymer concentration at the I-N transition for PHIC in toluene at 25°C [21]. Curves are predictions with $M_L = 740$ g/mol nm and $P = 37$ nm [21] using equation-of-state parameters in Table 2.

all models give correlations of similar quality. The hard-sphere diameter for Model 1 is close to that for the hard spherocylinder in Model 3.

Fig. 3a shows the osmotic pressure of isotropic PHIC solutions in toluene at 25°C. Curves are the fit by Model 2 for molecular weights 133 000 and 244 000. Itou et al. [20] also report data for PHIC with $M = 32\,000$. However, we were not able to correlate simultaneously the data for all three molecular weights of PHIC using a unique set of equation-of-state parameters, partly because the PHIC with $M = 32\,000$ is more polydisperse than the others [20]. In addition, molecular weight 32 000 may not be large enough for our assumption that equation-of-state parameters are independent of molecular weight for PHIC in toluene.

Fig. 3b shows the concentration of polymer at the I–N transition for PHIC in toluene at 25°C. Curves are predictions with $M_L = 740$ g/mol nm and $P = 37$ nm [21]. All

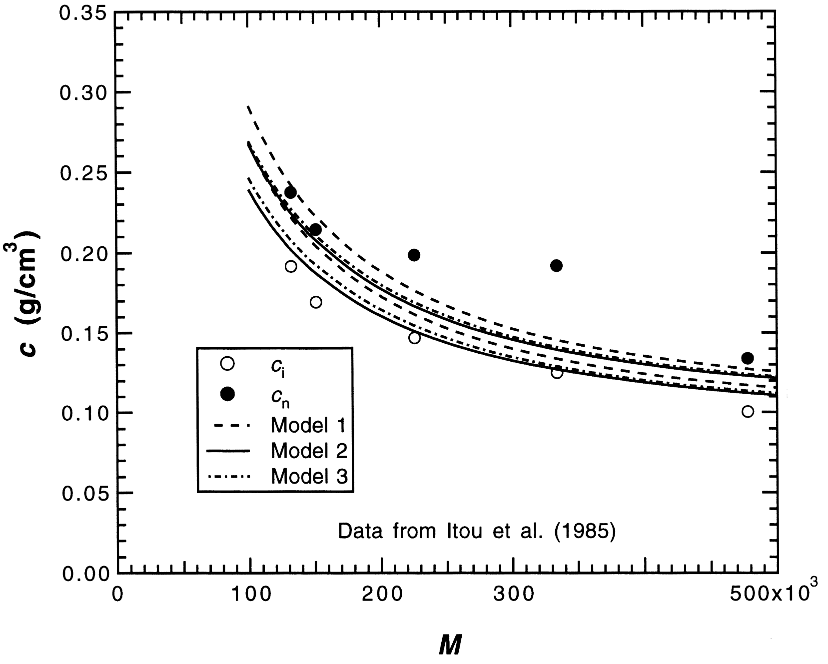

Fig. 4. Polymer concentration at the I–N transition for polysaccharide schizophyllan in water at 25°C [22,23]. Curves are predictions with $M_L = 2150$ g/mol nm and $P = 200$ nm [23] using equation-of-state parameters in Table 3.

models predict similar polymer concentrations at the I–N transition that are slightly lower than experiment. At the I–N transition, experiment shows that the difference in the concentration of PHIC between the isotropic and nematic phases is smaller in toluene than in DCM shown in Fig. 2b. For PHIC in toluene, all models predict the difference in the concentration of PHIC between the isotropic and nematic phases in agreement with experiment.

4.3. Polysaccharide schizophyllan in water

Finally, we compare Models 1–3 with experiment for an aqueous solution of polysaccharide schizophyllan [22,23] that has a rigid helical conformation in water characterized by $M_L = 2150$ g/mol nm and $P = 200$ nm at 25°C [23]. For aqueous solutions of polysaccharide schizophyllan at 25°C, Table 3 gives the equation-of-state parameters regressed from the sedimentation equilibrium data of isotropic solutions measured by Van and Teramoto [22]. Similar to the equation-of-state parameters for PHIC in toluene shown in Table 2, the hard-sphere diameter for Model 1 is close to that for the hard spherocylinder for Model 3. All models correlate the data of Van and Teramoto with similar quality.

Table 3
Equation-of-state parameters for polysaccharide schizophyllan in water at 25°C

	Model 1	Model 2	Model 3
d (Å)	22.2	10.7	21.4
r/M (mol/g)	0.000162	0.000700	0.000172^b
%rms^a	4.0	4.1	3.3

[a] Percent root-mean-square relative deviations.
[b] x/M (mol/g).

In aqueous solutions of polysaccharide schizophyllan, the anisotropic phase is not the nematic phase, but the cholesteric phase. However, the cholesteric phase is very similar to the nematic phase; we therefore neglect the difference between the nematic and cholesteric phases [28]. Fig. 4 shows the polymer concentration at the isotropic–anisotropic transition for polysaccharide schizophyllan in water at 25°C [23]. Data are for the isotropic–cholesteric transition [23] and curves are the predictions for the I–N transition. The scatter in the data may be partly due to the polydispersity effect because polysaccharide schizophyllan [23] shown in Fig. 4 is more polydisperse than PHIC shown in Figs. 2 and 3 [21]. For lyotropic polymer liquid crystals, polydispersity has a large effect on the isotropic–anisotropic transition [23].

5. Conclusions

To predict the isotropic–nematic (I–N) transition of lyotropic polymer liquid crystals, Parsons-type scaling and the Onsager theory were combined with the equation-of-state for hard-sphere-chain fluids of Chapman et al. [10] and that of Hu et al. [13] The primary difference between these equations lies in the second virial coefficient. The equation of Chapman et al. gives a second virial coefficient larger than that of Hu et al. for $r > 1$ where r is the number of segments per chain. These models were first compared with the computer simulation by Wilson and Allen [18] for a nearly rigid semi-flexible hard-sphere chain consisting of seven segments. The equation of Hu et al.

gives the I–N transition concentration and pressure in good agreement with the computer simulation by Wilson and Allen [18].

For real semi-flexible polymers, we follow the procedure of DuPré and Yang [3,5] that introduces chain flexibility into the orientational entropy using the Khokhlov–Semenov theory of persistent chains [19]. This procedure requires the persistence length to specify the extent of chain flexibility. The persistence length affects only the Helmholtz energy of the nematic phase.

The equations of Chapman et al. (Model 1) and Hu et al. (Model 2) were also compared with experiment for two binary polymer solutions containing poly(hexyl isocyanate) (PHIC) and for another solution that contains polysaccharide schizophyllan. For comparison, calculations were also made using the theory of DuPré and Yang [3,5] (Model 3) for hard spherocylinders [4] based on Parsons scaling. To provide a fair comparison among these models, we first regressed the equation-of-state parameters that represent the size of polymer from experimental osmotic-pressure data for isotropic solutions. For each solvent-polymer pair, we used the reported persistence length regressed from intrinsic-viscosity data using the wormlike-chain theory. The concentration of polymer at the I–N transition was then predicted as a function of polymer molecular weight.

In the isotropic phase, Models 1–3 correlate well the osmotic pressure and the first derivative of osmotic pressure with respect to polymer concentration. There is no appreciable difference in the predicted polymer concentration at the I–N transition. However, as shown in Fig. 2b for PHIC in dichloromethane, the differences among Models 1–3 may become apparent for low-molecular-weight polymers.

Considering the large uncertainty in the persistence length of polymers, agreement of theory with experiment is encouraging. For Parsons-type scaling used in this work, for sufficiently large polymers, the expression for the compressibility factor of the isotropic phase is not important as long as the model is capable of correlating the osmotic pressure of isotropic solutions.

Acknowledgements

This work was supported by the Director, Office of Energy Research, Office of Basic Energy Sciences, Chemical Sciences Division of the US Department of Energy under Contract no. DE-AC03-76SF0098. Additional funding was provided by E.I. du Pont de Nemours and Co. (Philadelphia, PA) and Koninklijke Shell (Amsterdam, The Netherlands) and by the Donors of the Petroleum Research Fund administered by the American Chemical Society.

References

[1] Ciferri A, editor. Liquid crystallinity in polymers: principles and fundamental properties. New York: VCH, 1991.
[2] Odijk T. Macromolecules 1986;19:2313.
[3] Vroege GJ, Lekkerkerker HNW. Rep Prog Phys 1992;55:1241.
[4] Lee SD. J Chem Phys 1987;87:4972.
[5] DuPré DB, Yang SJ. J Chem Phys 1991;94:7466.
[6] Hentschke R. Macromolecules 1990;23:1192.
[7] Parsons JD. Phys Rev A 1979;19:1225.
[8] McGrother SC, Williamson DC, Jackson G. J Chem Phys 1996;104:6755.
[9] Wertheim MS. J Chem Phys 1987;87:7323.
[10] Chapman WJ, Jackson G, Gubbins KE. Mol Phys 1988;65:1057.
[11] Chiew YC. Mol Phys 1990;70:129.
[12] Boublík T, Vega C, Diaz-Peña M. J Chem Phys 1990;93:730.
[13] Hu Y, Liu H, Prausnitz JM. J Chem Phys 1996;104:396.
[14] Song YH, Lambert SM, Prausnitz JM. Macromolecules 1994;27:441.
[15] Dickman R, Hall CK. J Chem Phys 1988;89:3168.
[16] Vega C, Lago S. J Chem Phys 1994;100:6727.
[17] Williamson DC. Physica A 1995;220:139.
[18] Wilson MR, Allen MP. Mol Phys 1993;80:277.
[19] Khokhlov AR, Semenov AN. Physica A 1982;112:605.
[20] Itou T, Sato T, Teramoto A, Aharoni SM. Polymer J 1988;20:1049.
[21] Itou T, Teramoto A. Macromolecules 1988;21:2225.
[22] Van K, Teramoto A. Polymer J 1985;17:409.
[23] Itou T, Van K, Teramoto A. J Appl Polym Sci, Polym Symp 1985;41:35.
[24] Williamson DC, Jackson G. Mol Phys 1995;86:819.
[25] Sato T, Teramoto A. Mol Cryst Liq Cryst 1990;178:143.
[26] Yu M, Liu Q. Macromolecules 1996;29:6928.
[27] Wilson MR. Mol Phys 1994;81:675.
[28] Chandrasekhar S. Liquid crystals. Cambridge: Cambridge University Press, 1977.